



OPEN ACCESS

EDITED BY

Abdul-Sattar Nizami,
Government College University, Pakistan

REVIEWED BY

Sanja Josip Armakovic,
University of Novi Sad, Serbia
Muhammad Shahbaz,
Hamad bin Khalifa University, Qatar
Alberto Pettinau,
Sotacarbo S.p.A., Italy

*CORRESPONDENCE

Tahir Asif,
✉ tahir.asif@uet.edu.pk
Yasser Fouad,
✉ yfouad@ksu.edu.sa

RECEIVED 21 November 2023

ACCEPTED 19 December 2023

PUBLISHED 15 January 2024

CITATION

Asif T, Noor F, Imran S, Mujtaba MA, Farooq M, Fouad Y, Kalam MA and Uddin GM (2024), Microwave-assisted transesterification of *Litchi chinensis* seed oil using extracted KOH from potato waste for sustainable development. *Front. Energy Res.* 11:1339601. doi: 10.3389/fenrg.2023.1339601

COPYRIGHT

© 2024 Asif, Noor, Imran, Mujtaba, Farooq, Fouad, Kalam and Uddin. This is an open-access article distributed under the terms of the [Creative Commons Attribution License \(CC BY\)](https://creativecommons.org/licenses/by/4.0/). The use, distribution or reproduction in other forums is permitted, provided the original author(s) and the copyright owner(s) are credited and that the original publication in this journal is cited, in accordance with accepted academic practice. No use, distribution or reproduction is permitted which does not comply with these terms.

Microwave-assisted transesterification of *Litchi chinensis* seed oil using extracted KOH from potato waste for sustainable development

Tahir Asif^{1*}, Fahad Noor¹, Shahid Imran¹, M. A. Mujtaba¹, Muhammad Farooq¹, Yasser Fouad^{2*}, M. A. Kalam³ and Ghulam Moeen Uddin¹

¹Faculty of Mechanical Engineering, University of Engineering and Technology, Lahore, Pakistan,

²Department of Applied Mechanical Engineering, College of Applied Engineering, Muzahimiyah Branch, King Saud University, Riyadh, Saudi Arabia, ³School of Civil and Environmental Engineering, FEIT, University of Technology Sydney, Sydney, NSW, Australia

The fast depletion of conventional fuel supplies has forced the world to find suitable substitutes to overcome the expected energy crisis. Fossil fuels also contribute to global warming because of their harmful emissions. Biofuels are sustainable and environment friendly. Biodiesel can be sourced from both edible and non-edible oils to replace fossil fuels. To avoid a shortage of food supply, it is preferred to produce biodiesel from non-edible oils. In this research, *Litchi chinensis* seed oil (LSO) is used as a feedstock to synthesize biodiesel employing transesterification using a microwave oven. The catalyst, potassium hydroxide (KOH), used in this research was extracted from potato waste. Sun-dried potato waste was converted into ash. The produced ash is then dissolved in distilled water, leading to a 34% yield of KOH. The transesterification achieves a 92.9% conversion rate under the conditions: 30% microwave power utilization, a catalyst loading of 15% (W/W), a stirring speed of 700 RPM, and a methanol concentration of 70% (V/V) with an 8-min reaction time. Response surface methodology (RSM), in comparison with artificial neural networks (ANNs), has been utilized for the optimization of biodiesel yield, giving efficient results with errors of 0.003% for RSM and 0.005% for ANN. Consequently, the study reports optimized biodiesel yields of 92.9% (experimental), 93.27% (RSM), and 92.40% (ANN). Physicochemical properties such as kinematic viscosity (4.4 mm²/s) at 40°C, density (875 kg/m³) at 15°C, cetane number (53.2), calorific value (38.8 MJ/kg), flash point (175°C), oxidative stability (6.1 h), and cold flow properties were determined with respect to the ASTM and EN standards. The findings reveal that biofuels primarily support Sustainable Development Goals (SDGs) 7 and 13, with the prime focus on “affordable and clean energy” and “climate action,” respectively.

KEYWORDS

Litchi chinensis, biodiesel, potato waste, response surface methodology and artificial neural network, microwave, sustainable environment

1 Introduction

For decades, petroleum has been the backbone of the industrialized society. Heavy dependence on petroleum is undeniable, as it is essential to produce liquid fuels, petrochemicals, road construction materials, packaging, and advanced medical technologies (Cormos et al., 2013; Cheng et al., 2021; Liu et al., 2022a; Kabeyi and Olanrewaju, 2022). Since the start of the industrial revolution in the late 18th and early 19th centuries, energy has been an essential factor in ensuring sustained economic growth and sustaining a rising living standard (Wang et al., 2022). The International Energy Agency (IEA) forecasts that by 2030, the global energy demand will be 50% more than it is today (Amran et al., 2020), with China and India being responsible for about half of the increase. Estimations suggest that the worldwide energy demand linked to transportation is anticipated to increase by over 25% from 2017 to 2040 (Yusoff et al., 2022). Four million barrels of oil leaked into the Gulf of Mexico during transportation that resulted in some harmful ecological and economic effects across the continent (Wang et al., 2023). Air pollution and the greenhouse effect produced by emissions from combustion engines have gained more attention recently. Many scientists agree that climate change is one of the most significant issues that our ecosystem is facing. The global surface temperature has risen by $\approx 0.2^\circ\text{C}$ per decade over the last 3 decades (Hansen et al., 2006). If the global average temperature rises by 2°C , millions of species may face death, and the lives of multiple humans could be at risk (Li et al., 2023).

Over the past decade, it has become evident that greenhouse gases, especially CO_2 , pose a significant threat to future generations by contributing to climate change and global warming. From 2020 to 2035, it has been predicted that more than 4 billion MT (metric tons) of CO_2 will be discharged into the environment (Yang et al., 2023). In Western countries, the transportation sector constitutes almost 30% of the overall energy consumption, with approximately one-third of this energy usage attributed specifically to light-duty vehicles (LDVs). Emissions released by cars running on fossil fuels have forced the European Union (EU) to propose a ban on the use of fossil-fuel cars starting 2035. Biofuels and e-fuels are possible alternatives to fossil fuels (Liu et al., 2022b). The increased global recognition of energy challenges has strengthened research efforts to explore the potential use of alternative and renewable sources of energy. Biodiesel is biodegradable and carbon-neutral by nature. Biodiesel can be synthesized from a range of sources such as edible oils (Li et al., 2023; Yang et al., 2023), non-edible oils (Moser, 2008; Liu et al., 2022b; Banković-Ilić et al., 2012; Silitonga et al., 2019), animal fats (Wang et al., 2023), waste cooking oil (WCO) (Degfie et al., 2019), and algae (Kan et al., 2023a). Over 60 countries around the world are utilizing biodiesel to cope with their energy challenges (Yusoff et al., 2021). Many countries are promoting the adoption of biodiesel to reduce their dependence on fossil fuels. Among potential candidates, edible oils like palm oil (PO) are promising due to their high oil yield for biodiesel synthesis. However, there is a growing interest in utilizing biodiesel sourced from non-edible crops as a future source for biodiesel production. This shift is aimed at reducing reliance on edible oils and reducing their long-term demands on the human food supply. Non-edible plants like *Jatropha curcas* (Azad et al., 2015), *Moringa* (Vijay Kumar et al., 2019), and mahua (Kan et al., 2023b) have

acquired significant consideration in this regard. Rahul et al. (2022) produced biodiesel using a microwave oven from non-edible silk-cotton seed oil.

The common advantage of biodiesel is its local origin, which decreases the reliance on imported petroleum. Biodiesel is also biodegradable, has an elevated flash point, and also possesses lubricity. It does not produce SO_x and has very low harmful emissions when compared to petroleum diesel. It also releases a reduced amount of carbon dioxide (Pandey et al., 2010). Ilkilic and Behçet (2010) evaluated the decrease of NO_x by 19%, CO by 22%, and CO_2 by 13% using biodiesel blends as compared with commercial diesel (Zhang et al., 2000; Duan et al., 2007).

Several feedstocks containing edible and non-edible oils are applicable to synthesize biodiesel. Researchers are more focused on using non-edible oils for sourcing biofuels to avoid a shortage of the food supply chain. *Litchi chinensis* is a significant fruit dispersed over various regions of the world, largely in subtropical areas. It is a common fruit found in southeast Asia. The by-products and waste of *Litchi chinensis* contain *Litchi chinensis* husks and seeds. Prior research on the biochemical processes of this fruit has been primarily focused on its pericarp because it carries an abundance of potential antioxidants. These antioxidants have been utilized for their medicinal properties over an extended period (Azad et al., 2015; Vijay Kumar et al., 2019). The seed from *Litchi chinensis* was examined for its oil production, fatty acids, and tocopherols. The amount of oil extracted from *Litchi chinensis* seeds with hexane is up to 3.2%. *Litchi chinensis* seed oil has been characterized by the availability of higher contents of dihydrosterculic acid (46.9%) and oleic acid (29.3%). The production of *Litchi chinensis* in the world is 2.11 million tons, of which 95% is produced in Asia. The highest producers of *Litchi chinensis* are China, India, Taiwan, and Vietnam.

Catalysts play a substantial role in boosting and streamlining chemically catalyzed reactions (Rizwanul et al., 2020). They are classified into three primary categories: 1) homogeneous, 2) heterogeneous, and 3) enzyme-based catalysts. Homogeneous catalysts (i.e., NaOH and KOH) are mostly utilized in biodiesel production. They are cost-effective, readily accessible, and capable of yielding a significant amount of biodiesel in a short period (400 times faster than acid catalysts) (Fukuda et al., 2001). KOH is a stronger base than NaOH, as it releases OH^- ions readily. It also rapidly dissolves in methanol and glycerin. Due to these reasons, researchers prefer to utilize KOH in the biodiesel synthesis process.

KOH can be extracted from vegetables rich in potassium, for example, spinach, banana stems, and potatoes. The potassium salts are transformed into potassium oxide, which is then converted to KOH. The extracted KOH is much cheaper than the commercially available potassium hydroxide. The literature is not enough on how to utilize potash extracted from biomass resources, as biodiesel production from alkaline-based biodiesel is more common (Efeovbokhan et al., 2016).

Potatoes are one of the most concentrated sources of potassium, surpassing other commonly recognized high-potassium foods like bananas, oranges, and broccoli. They have a diverse array of vitamins and minerals, especially potassium, magnesium, and iron. Across all potato varieties, potassium leads to the highest content among the minerals they offer, and they remain an

economical option. In particular, white potatoes come at nearly half the cost of most other vegetables, rendering them a more cost-effective means of obtaining potassium (Beals, 2019). Ahmad et al. (2023) produced biodiesel with extracted KOH from plantain stems using WCO as a feedstock.

The response surface methodology model is an important technique for the optimization of biodiesel yield (Fetimi et al., 2022). The optimal conditions for the transesterification reaction are calculated with the use of RSM (Ofoefule et al., 2019). The RSM employs the central composite design (CCD) to improve process variables such as oil/methanol volume ratio or molar ratio, concentration of the catalyst, time for the reaction to be carried out, and temperature of the reaction for optimal production of biodiesel (Helmi et al., 2021). The fundamental benefit of the RSM is its capacity to decrease experimental observations, which is important to develop statistically significant results (Chung et al., 2022). The RSM is used to optimize the conversion of vegetable oils to biofuels, i.e., sesame oil (Betiku and Adepoju, 2013), *Moringa oleifera* oil (Amini et al., 2008), rape seed oil (Yuan et al., 2008), and cotton seed oil (Zhang et al., 2010). Milano et al. (2018) applied transesterification to synthesize biodiesel from a blend of WCO and *Calophyllum inophyllum* oil using a microwave oven. The RSM was implemented to achieve a biodiesel yield of 97.65% in 9.15 min. This methodology includes enhanced biodiesel yields, accelerated chemical reactions, and reduced overall energy consumption.

Machine and deep learning methodologies, along with specific algorithms, have modernized many industrial sectors, especially the optimization of biodiesel production. The capabilities of these algorithms are superior to traditional machine learning methods, resulting in a substantial advancement in their efficiency, adaptability, and overall performance across various applications. These methodologies empower deep neural networks to adapt and improve their operational efficacy, particularly when confronted with shifting data patterns, non-static environments, or unforeseen and evolving variables. This adaptability permits them to continuously optimize and refine their performance over time (Zhang et al., 2020). The integration of these algorithms with optimization techniques presents a successful approach in managing complicated connections among input reaction parameters and desired output parameters, effectively balancing factors like production yield and product quality in complex systems (Wu and Zhao, 2020).

Artificial neural network (ANN) practice has grown in popularity recently due to its computational efficiency (Jalali et al., 2021). ANN is proficient in solving complex and complicated non-linear problems. It is used for nonlinear function calculation, data categorization, and nonparametric regression (Lin et al., 2020). For the production of biodiesel, ANN uses artificial intelligence to optimize esterification and transesterification reactions (Amini et al., 2008; Yuan et al., 2008). Kolakoti (2020) applied the ANN technique to achieve a maximum biodiesel yield of 92.17% and found it to be accurate for predicting the biodiesel yield. ANN is used with RSM to optimize the yield of biodiesel because ANN can handle nonlinear relationships and complex patterns within data, complementing RSM's ability to model and optimize processes based on experimental data (Maran and Priya, 2015). The ANN and RSM, when employed together,

have been demonstrated to be effective methodologies for the process modeling of biofuels, which can save energy, money, and time (Rajendra et al., 2009).

Biodiesel can be synthesized using modern tools that are more efficient in terms of energy. For instance, microwave technology can replace the conventional heating system, which significantly reduces the required power and shortens the reaction duration. Adoption of the microwave system in the transesterification process will accelerate biodiesel synthesis and decrease reaction time. This acceleration is achieved by accelerated heat transfer and improved chemical reactions, resulting in 48% energy savings (Fattah et al., 2014a; Fattah et al., 2014b; Palma et al., 2020).

There is limited literature available on the extraction of potassium hydroxide (KOH) from potato waste. The implications of RSM and ANN for optimizing the biodiesel yield from *Litchi chinensis* seed oil have not been investigated earlier. In the present study, KOH as a catalyst was extracted from potato waste, and a modified microwave was used as the biodiesel reactor for LSO biodiesel production. The RSM utilizing CCD and ANN methodologies was used to optimize the impact of catalyst (KOH) concentration (wt%), methanol/oil concentration (%V/V), reaction time (minutes), and stirring speed (RPM). The yield of biodiesel was enhanced using former methodologies. The study also includes the validation of the physicochemical properties of the synthesized biodiesel. The outline of this study is as follows: materials and methods are explained in Section 2, while results and discussion are reported in Section 3. The conclusion follows in Section 4.

2 Materials and methods

A microwave oven (DW-295) and stirrer were used in this research; all other chemicals employed were of analytical grade.

2.1 Extraction of the catalyst

2.1.1 Conversion of potato waste to ash

Ten kilograms of potato waste was initially cleaned to eliminate any debris and dust particles, followed by multiple washes with deionized water. Afterward, the cleaned potato waste was placed for sun drying for 72 h, resulting in 2 kg of dried potato waste. The sample (2 kg) was converted to powder by using a grinder. Then, it was subjected to a 2-h burning process in a furnace set at 600°C for the removal of carbonates. The calcination process at 600°C indeed induces the breakdown of organic compounds present in the potato waste powder. During calcination, the high temperature causes the elimination of organic compounds such as cellulose, starch, sugars, and carbon-based compounds present in the potatoes. It leads to the potential release of volatile elements like water vapor and carbon dioxide. The ash was found to be 16% (calculated by Eq. 1). The catalyst extraction methodology from potato waste is shown in Figure 1.

$$\% \text{Age of ash recovered} = \frac{\text{Weight of ash recovered}}{\text{Weight of dried potatoes sample}} \times 100. \quad (1)$$

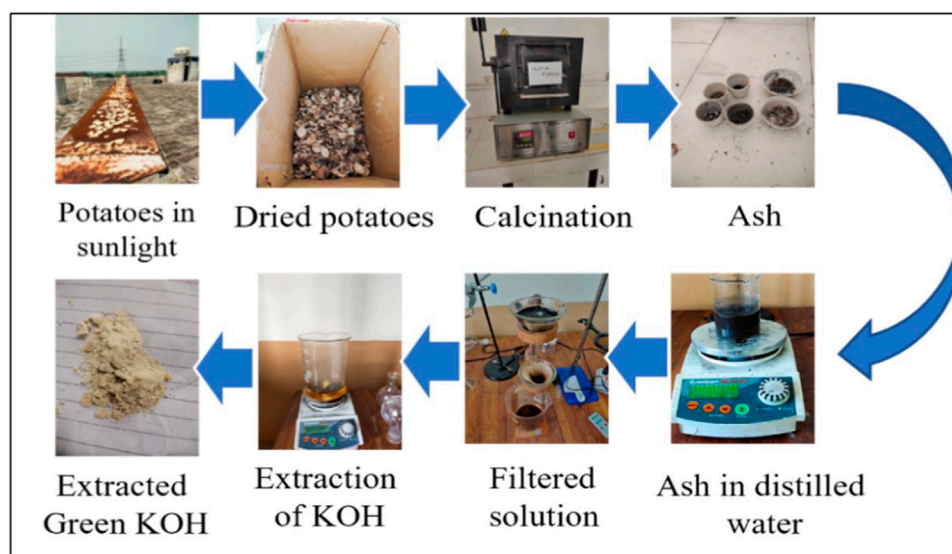


FIGURE 1
Flow diagram for the extraction of KOH from potato waste.

2.1.2 KOH extraction from potato waste ash

KOH is produced by hydrating K_2O from ash sample. A 20 g portion of the prepared ash was measured and dissolved in distilled water (10 mL/g) in a 500 mL beaker. The prepared solution was put on a hot plate, and it was continuously stirred for a duration of 2 h at 60°C . Then, the solution was filtered and dried by heating. The recovered KOH was 34% calculated by Eq. 2.

$$\% \text{Age of KOH recovered} = \frac{\text{Weight of KOH recovered}}{\text{Weight of ash sample}} \times 100. \quad (2)$$

2.2 Pretreatment of *Litchi chinensis* seed oil

The acid value of *Litchi chinensis* seed oil was calculated by Eq. 3. The free fatty acid (FFA) value was then calculated as [acid value (AV)]/2 (Lin et al., 2020; Tran-et al., 2020; Laskar et al., 2022).

$$AV = (56.1 \times V \times N)/W. \quad (3)$$

where N denotes the normality of KOH, W indicates the weight of utilized LSO, and V is the combined volume of potassium hydroxide and distilled water.

If the FFA composition of *Litchi chinensis* seed oil is higher than 2%, then the feedstock has to be improved with H_2SO_4 through a process called esterification. The esterification is done by using H_2SO_4 and methanol at 1.5% and 70% volume of oil, respectively. The stirring speed (600 RPM) and temperature (60°C) were maintained for 2 h (Ighose et al., 2017; Milano et al., 2018; Ishola et al., 2019). Once the esterification is done, then transesterification is carried out.

2.3 Experimental setup for the production of biodiesel

The experimental setup in the schematic form is displayed in Figure 2. The experimental setup for biodiesel synthesis consists of a round bottom flask that is placed in the microwave oven and having an extended neck with three openings. In one opening, a glass condenser is attached, the central opening carries the glass stirrer, and the third opening is used to monitor the temperature and for charging the raw material. A 500 mL separating funnel is utilized to separate the layers. The characterization of biodiesel was done by using GCMS and that of the catalyst by using Fourier transform infrared spectroscopy (FTIR). Table 1 illustrates the specifications of the microwave oven used in this study.

2.4 Biodiesel production from *Litchi chinensis* seed oil

LSO was used to synthesize biodiesel via a microwave-assisted transesterification process. Catalyst concentration, methanol concentration, time, and stirrer speed are the four important operating parameters that influence the biodiesel yield. The power of the microwave oven (30%) and time for the reaction are adjusted in such a way that the temperature is maintained at 64°C . After transesterification is completed, the solution was kept for 8 h to separate glycerin from the sourced biodiesel.

Glycerin was collected from the separating funnel. The resulting biodiesel was washed up using hot distilled water to eliminate any suspended glycerin particles and soap. After washing, biodiesel was collected in a separate beaker, and water contents were eliminated by heating at 100°C for half an hour. The ranges of operating parameters are given in Table 2.

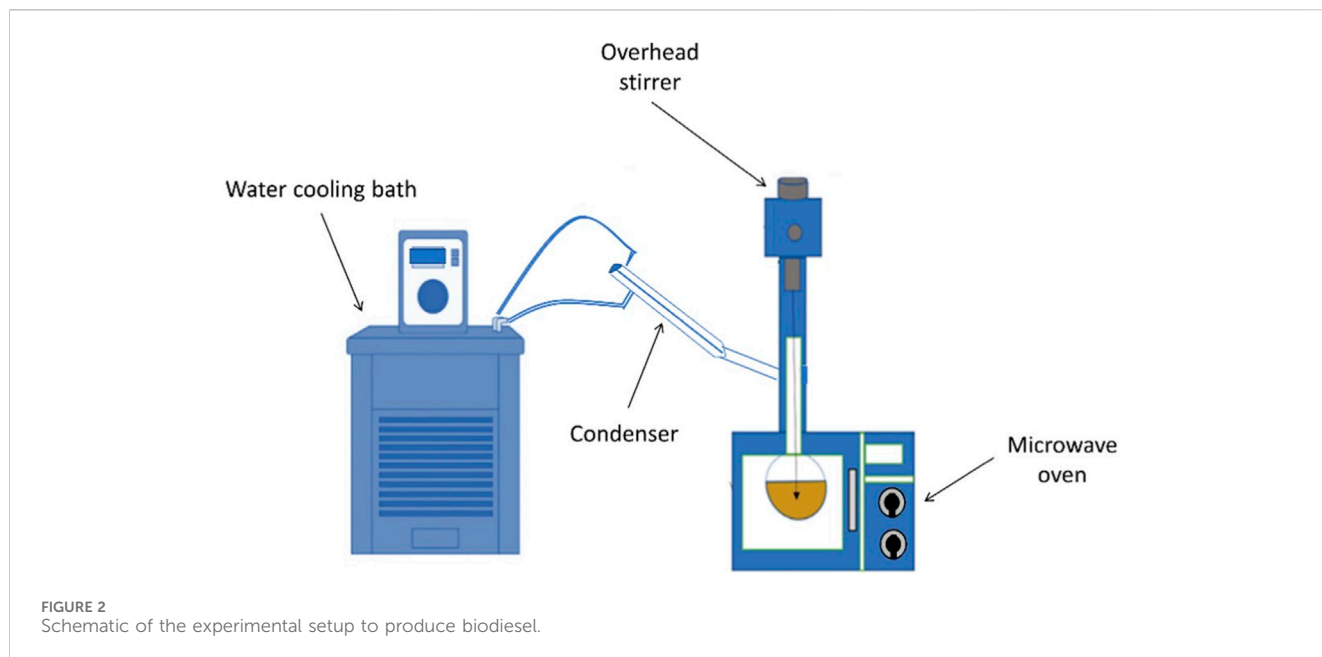


TABLE 1 Specifications of the microwave oven.

Specification	DW-295
Capacity	20 L
Maximum power	700 W (can operate at 10%, 30%, 50%, 80%, 100%)
Round bottom flask material	Borosilicate glass
Rated voltage	230 V
Rated frequency	50 Hz
Frequency of microwave	2450 MHz

TABLE 2 Ranges of operating variables.

Operating variable	Units	Range
Catalyst concentration	W/W%	10–15
Stirring speed	RPM	500–700
Reaction time	Minutes	5–8
Methanol concentration	%V/V	40–70

2.4.1 Yield optimization of biodiesel

Operating variables were optimized using Design Expert 13.0 to obtain the maximum possible biodiesel yield. Four independent parameters for optimization include catalyst concentration (wt%), methanol concentration (vol%), time for reaction (minutes), and the speed of stirring (RPM). To verify RSM output, an ANN was used. In Figure 3, the microwave-assisted transesterification reaction is illustrated.

2.4.2 ANN method

ANN is analogous to that of neuronal networks within the human brain. It is used to verify RSM yields and predict the

optimum yield. Synaptic weights are typically used to link neurons in ANN. The optimal response is achieved by training neurons according to their given function (for example, tansig or purelin). Neurons have the capacity to store information.

The feedforward backpropagation ANN was configured with the trainlm training algorithm, the learnGDM adaptation learning function, and the mean square error performance function. The standard ANN architecture consists of seven neurons distributed across three input layers, three hidden layers, and the last output layer. Transfer functions like logsig, tansig, and purelin are implemented on these levels. The biodiesel yield is the output of 17 iterations of independent variables of this model. The MATLAB R2019a (The MathWorks, Inc., Natick, USA) had been utilized to create the ANN.

2.4.3 Statistical data analysis

The implementation of the RSM and ANN is presented by the coefficient of determination (denoted by R^2), mean square error (denoted by MSE), root mean square error (denoted by RMSE), and finally, standard error of prediction (denoted by SEP). These terms are calculated, respectively, by Eq. 4, Eq. 5, Eq. 6, and Eq. 7 (Kolakoti, 2020; Maran and Priya, 2015).

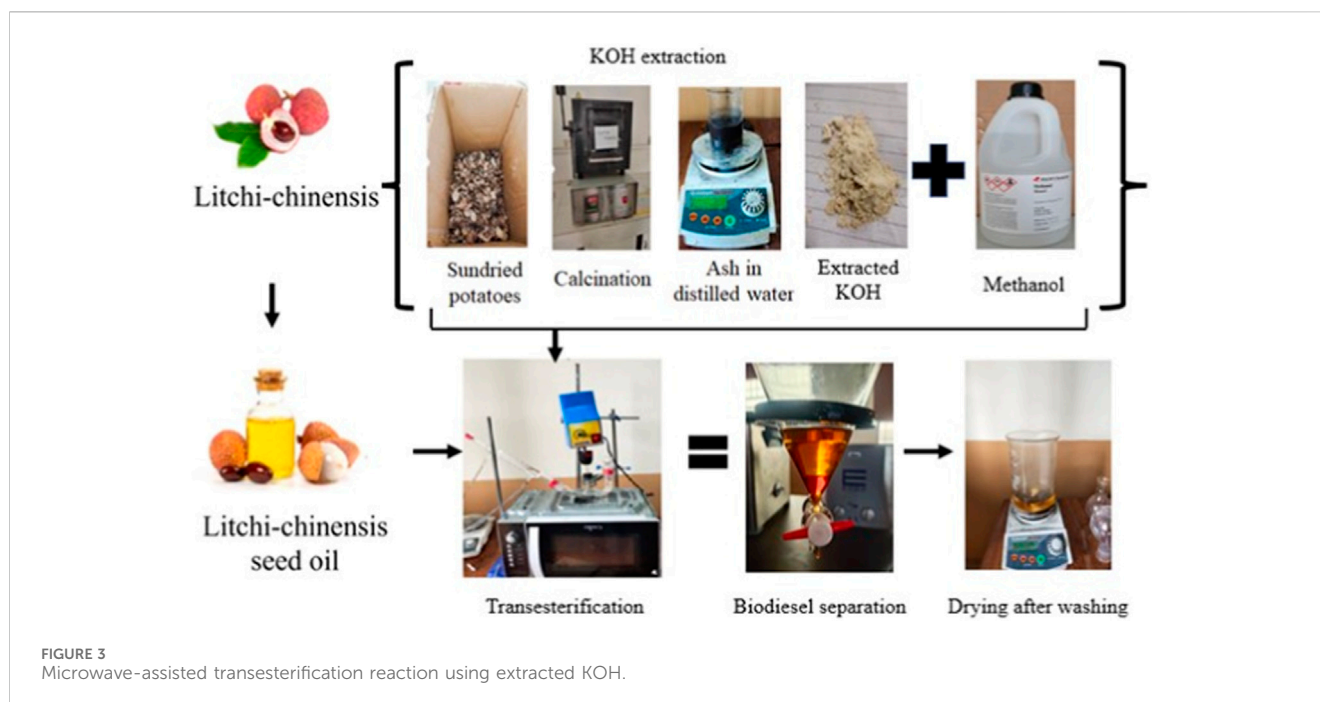
$$R^2 = 1 - \frac{\sum_{i=1}^n (ye - yp)^2}{\sum_{i=1}^n (yp - yavg)^2}, \quad (4)$$

$$MSE = \frac{\sum_{i=1}^n (ye - yp)^2}{n}, \quad (5)$$

$$RMSE = \left(\frac{1}{n} \sum_{i=1}^n (ye - yp)^2 \right)^{\frac{1}{2}}, \quad (6)$$

$$SEP = \frac{RMSE}{yavg} \times 100, \quad (7)$$

where n corresponds to the number of points, ye represents the actual value, yp represents the predicted value, and $yavg$ represents the average of the actual values.



2.5 FTIR of KOH

FTIR of KOH was performed with the help of a PerkinElmer Spectrum One with wavenumbers ranging from 500 to 4,000 cm^{-1} . In FTIR, infrared light passes through a sample. The light absorbed by the sample is evaluated as a function of the frequency of light. This provides information about the vibrational modes of the molecules in the sample and can be used to identify the functional groups.

2.6 GCMS analysis of biodiesel

The GCMS evaluation of biodiesel sourced from LSO was performed by operating the Shimadzu GCMS-QP2010. For the analysis, a Shimadzu Model QP2010 equipped with a capillary column (30 m length \times 0.25 mm OD \times 0.25 μm film thickness) was utilized, with helium as the carrier gas. The flow rate was maintained at 1.5 mL/min. The volume of the injected sample was 1 μL . The oven temperature was set at 60°C, maintained for 2 min, then increased from 60°C to 200°C at the rate of 10°C/min, and finally increased from 200°C to 240°C at the rate of 5°C/min, where it was kept for 7 min. The post-run was done at 255°C and maintained there for 0.5 min.

2.7 Characterization techniques for biodiesel

The physicochemical properties of the synthesized biodiesel have been evaluated using the following techniques and methods as mentioned in Table 3.

3 Results and discussion

This section includes the analysis of extracted KOH using FTIR. Additionally, optimization studies are conducted utilizing both RSM and ANN techniques. The precision and suitability of both models are analyzed based on statistical data. The properties of the biodiesel derived from *Litchi chinensis* seed oil are evaluated, and finally, the composition of the resulting biodiesel is discussed. Furthermore, the energy consumption by regular transesterification with that by using a microwave oven is compared.

3.1 FTIR of pure and extracted KOH

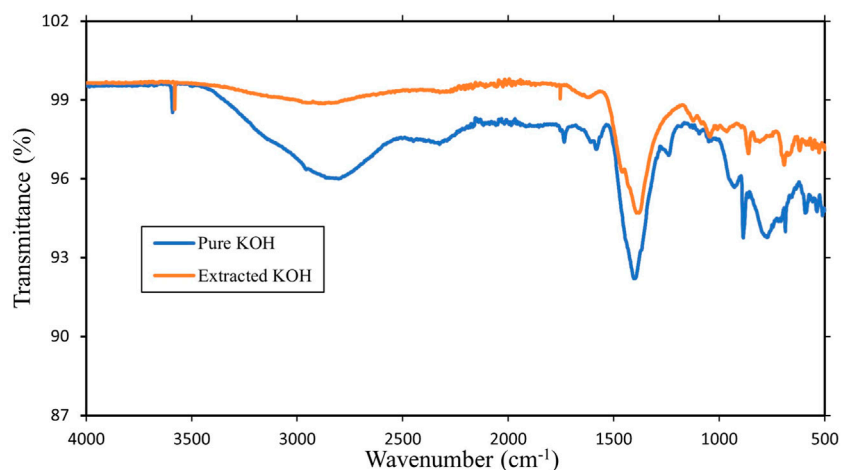
The wavenumber deployed is in the range of 500–4,000 cm^{-1} . The FTIR analyses (see Figure 4) of pure KOH and that of extracted KOH are represented as blue and orange patterns, respectively. Peaks at 3,591 cm^{-1} and 1,405 cm^{-1} represent the molecular transmittance of pure KOH for OH strengthening in the hydroxyl group. Peaks at 1,733 cm^{-1} and 1,583 cm^{-1} detect H₂O absorption in pure KOH, while those at 886 cm^{-1} identify the bond between KO in pure KOH. Other peaks that are present in the FTIR spectrum of KOH include those corresponding to bending vibrations of the O-H bond and vibrations of the K-O-H bond. The slight deviation between the pure KOH and extracted KOH patterns (Figure 4) is due to the presence of other impurities.

3.2 *Litchi chinensis* seed oil pretreatment

The FFA composition of the *Litchi chinensis* seed oil was calculated, and it was noted that the FFA composition was 2.5%, i.e., higher than 2%, so the oil was pretreated to reduce its FFA. The FFA was decreased to 0.5049 mg KOH/g. It is observed that the FFA proportion of the LSO

TABLE 3 Characterization techniques for physicochemical properties of biodiesel.

Property	Units	Test method	Technique/equipment	Model name
Density at 15°C	kg/m ³	ASTM D4052	Mettler Toledo density meters	DMA 4500
Kinematic viscosity at 40°C	mm ² /s	ASTM D445	Efflux viscometer	Redwood No. 1
Acid value	mg KOH/g	ASTM D664	Titration	—
Cetane no.		ASTM D4737	Cetane rating unit	CFR F5
Calorific value	MJ/kg	ASTM D240	Bomb calorimeter	Parr 6400
Flash point	°C	ASTM D93	Automatic tester for flash point	Pensky-Martens
Oxidative stability	h	EN 14112	Rancimat method	Metrohm 893
Cloud point	°C	ASTM D2500	Automatic tester used for pour point and cloud point	Anton Paar CPP 5Gs
Pour point	°C	ASTM D97		
Cold filter plugging point	°C	ASTM D6371	Cold filter plugging point tester	Callisto 100

FIGURE 4
FTIR of pure and extracted KOH.

after esterification had been lowered to less than 2%, implying that now the oil can be utilized for transesterification for biodiesel production.

3.3 Biodiesel yield optimization using RSM

Since the biodiesel output is dependent on the operating parameters, RSM creates an interaction between the parameters to find the best possible arrangement for biodiesel production. Consider four reactant inputs: the methanol concentration (A), the concentration of the catalyst (B), the time for the reaction to be carried out (C), and the stirring speed (D). For 29 different tests, *Litchi chinensis* seed oil was used to produce biodiesel.

$$\begin{aligned} \text{Yield} = & +87.59 + 1.18A + 0.3129B + 1.53C + 1.33D + 0.6744AB \\ & - 0.2669AC - 0.9356AD + 1.74BC + 0.1169BD \\ & + 0.0006CD \end{aligned}$$

(8)

The predictions are made considering the outcomes for the provided levels of each factor by using Eq. 8 in the coded factors. +1 and -1 have been termed as the high and low levels of the factors, respectively. The comparison of the factor coefficients for detecting the relative effect of the factors shows that the coded equation is feasible. The matrix for experimentation, established by the Design-Expert software that involves CCD arrangement, and the results are listed in Table 4.

3.3.1 Validity of the RSM model

ANOVA is a useful statistical tool for validating yields as represented in Table 5. The model is significant as the model's F-value comes out as equal to 125.47. The *p*-value (0.0001) indicates that there is a chance of 0.01% that the F-value that is this much larger comes out because of noise. The "Prob > F" outcomes smaller than 0.0500 indicate that this model is considered significant. For the current state, A, B, C, D, AB, AC, AD, and BC (terms) are considered significant.

TABLE 4 Experimental design to optimize biodiesel yield derived from LSO.

A: Run	B: Methanol/oil, vol%	C: Catalyst concentration, Wt.%	D: Reaction time, minutes	E: Stirring speed, RPM	F: Actual yield%	G: Predicted yield%
1	40	10	5	700	88.85	88.85
2	55	12.5	6.5	400	85	84.94
3	40	15	5	700	84.8	84.89
4	40	10	8	700	88.9	88.98
5	25	12.5	6.5	600	85.4	85.22
6	40	15	8	700	91.89	91.96
7	55	12.5	3.5	600	85	84.52
8	85	12.5	6.5	600	90.3	89.96
9	55	12.5	6.5	600	87	87.59
10	55	12.5	6.5	600	87.29	87.59
11	55	12.5	6.5	600	87.7	87.59
12	40	10	8	500	85	84.69
13	70	15	5	500	86.2	86.26
14	55	17.5	6.5	600	88.77	88.22
15	40	15	8	500	87	87.2
16	55	7.5	6.5	600	86.55	86.97
17	55	12.5	9.5	600	91.2	90.66
18	55	12.5	6.5	600	87	87.59
19	70	10	8	700	87.77	87.59
20	70	15	5	700	87	87.27
21	55	12.5	6.5	600	87.1	87.59
22	70	10	5	700	88.6	88.53
23	70	15	8	500	92.3	92.26
24	70	15	8	700	92.9	93.27
25	70	10	8	500	87	87.05
26	70	10	5	500	88.1	87.99
27	40	15	5	500	80	80.13
28	55	12.5	6.5	800	90.75	90.24
29	40	10	5	500	84.8	84.56

p -values higher than 0.1000 reveal that the model terms are not considered significant. The “lack of fit” F-value of 2.15 shows the non-significance of the lack of fit as compared to the pure error. A possibility of 24.04% occurs because this large a value of the “lack of fit” is due to noise. So, the non-significance of the “lack of fit” is better, and the model is fit. Figure 5 refers to the actual *versus* predicted yield in percentage.

The “Pred R^2 ” of 0.9707 is in practical arrangement with the “Adj R^2 ” value of 0.9780, which indicates that the difference is smaller than 0.2. The signal-to-noise ratio was calculated using “Adeq Precision.” The signal-to-noise ratio of 52.725 specifies a

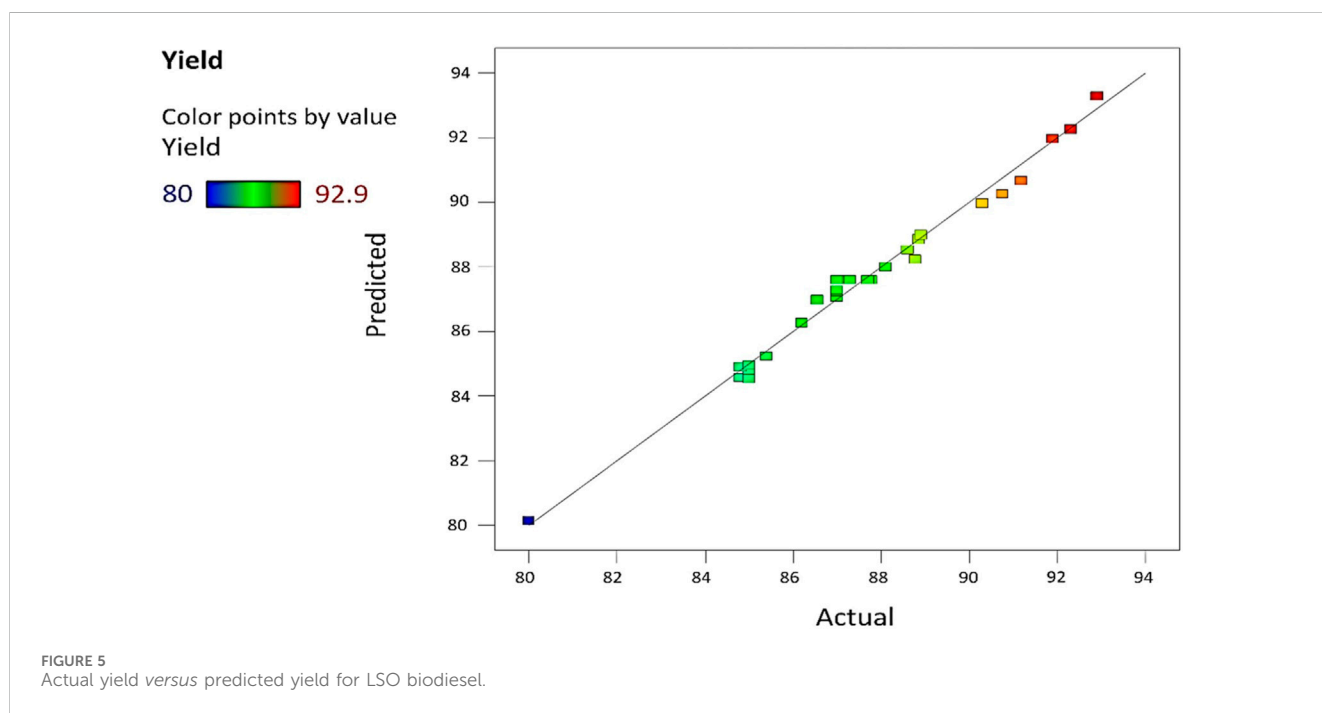
satisfactory signal, as it is appropriate above 4. The design space can be navigated by this model.

3.3.2 Effect of operating variables on the biodiesel yield

This section describes the impact of operating variables such as methanol/oil concentration, amount of catalyst utilized, reaction speed, and time for the reaction as shown in Figure 6. Figure 6A exhibits the combined impact of the methanol/oil volumetric ratio and catalyst content on the yield of biodiesel; the other two operating parameters—time for reaction and reaction speed—have been kept constant at 6.5 min and 600 RPM, respectively. It can be noted from

TABLE 5 Results of ANOVA based on CCD.

Source	Sum of squares	Degree of freedom	Mean square	F-value	p-value	
					Prob > F	
Model	205.49	10	20.55	125.47	<0.0001	Significant
A: Methanol/oil (vol%)	33.68	1	33.68	205.64	<0.0001	
B: Catalyst concentration	2.35	1	2.35	14.35	0.0013	
C: Reaction time	56.46	1	56.46	344.73	<0.0001	
D: Stirring speed	42.16	1	42.16	257.44	<0.0001	
AB	7.28	1	7.28	44.43	<0.0001	
AC	1.14	1	1.14	6.96	0.0167	
AD	14.01	1	14.01	85.52	<0.0001	
BC	48.20	1	48.20	294.30	<0.0001	
BD	0.2186	1	0.2186	1.33	0.2631	
CD	6.250E-06	1	6.250E-06	0.0000	0.9951	
Residual	2.95	18	0.1638			
Lack of fit	2.60	14	0.1858	2.15	0.2404	Not significant
Pure error	0.3465	4	0.0866			
Cor total	208.43	28				
Standard deviation	0.4047		R ²	0.9859		
Mean	87.59		Adj R ²	0.9780		
C.V.%	0.4620		Pred R ²	0.9707		
			Adeq Precision	52.725		



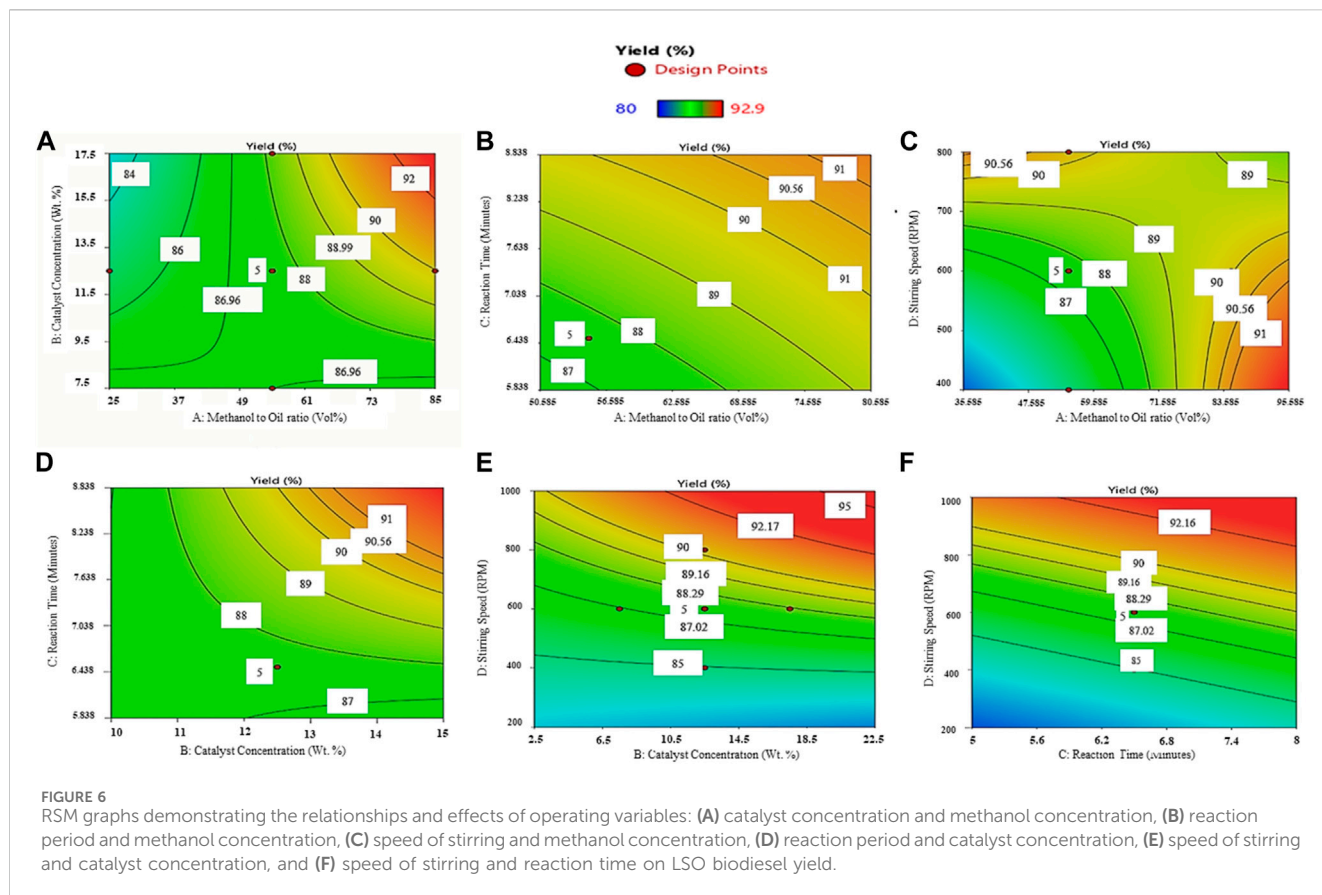


Figure 6A that the yield increases with increasing methanol/oil concentration and decreases with increase in the quantity of the catalyst. Increasing the content of methanol would shift the reaction equilibrium in favor of biodiesel production (Encinar et al., 2012). The achievement of the transesterification reaction is hindered when methanol content is low. Whereas an extra content of methanol leads to elevated costs associated with the recovery of methanol. Furthermore, at higher methanol levels, the separation of glycerol from biodiesel becomes more confronting. However, elevating methanol levels beyond the optimal limits resulted in decreased concentrations of reactants and catalysts (Zhang et al., 2018), and the retrieval of the solvent proved to be challenging when employing higher alcohol-to-oil ratios (Sahabdeen and Arivarasu, 2020). A high catalyst concentration can cause over-esterification, where excessive amounts of the catalyst cause the creation of by-products and lower the overall reaction yield. Increasing the catalyst concentration after a specified limit may increase viscosity of the sourced biodiesel because of emulsification (Patil and Deng, 2009).

The results of varying the methanol concentration and reaction time are displayed in Figure 6B. The other two operation parameters, that is, the catalyst concentration of 12.5 Wt% and the speed of 600 RPM, are kept constant. The yield is increased by increasing both dependent variables. The increased reaction yield is due to longer reaction times enabling complete conversion of reactants to products, and a higher methanol content provides more reactants to react. The lowest biodiesel efficiency was achieved initially, possibly resulting from

factors like an inadequate supply of oil for the transesterification reaction and inadequate contact time between the reactants (Gupta et al., 2020). Nevertheless, prolonging the reaction time beyond the optimal duration brings down the biodiesel yield, as it prompts a reversal of the reaction and the formation of soap. Hence, an excessive reaction time acts as a limiting factor for biodiesel yield and has an adverse effect on the biodiesel manufacturing process (Tamjidi et al., 2021).

Figure 6C illustrates the variation of two dependent variables—the methanol-to-oil ratio and stirring speeds—while the other two operating parameters—reaction time (6.5 min) and catalyst concentration (12.5 Wt%)—are kept constant. The yield significantly increases with increasing methanol/oil concentration and stirring speed. After reaching the optimal value of stirring speed, the yield starts decreasing. Improved mixing and mass transfer resulting from increased stirring speed contribute to better reaction kinetics and a greater yield. Conversely, the methyl ester yield declines beyond the optimal mixing speed value as the reaction reverses its nature once the reactants are depleted and products are produced, exerting control over the reaction (Elkelawy et al., 2019).

When the methanol/oil concentration is kept constant at 55 vol % and the stirring speed is set to 600 RPM, as depicted in Figures 6A, D, an increase in the catalyst concentration and reaction time leads to an increase in the yield. The yield of the reaction is significantly impacted by the reaction time. However, reactant depletion, saturation, and kinetic changes can all occur as reaction time increases, lowering the yield beyond the optimal value.

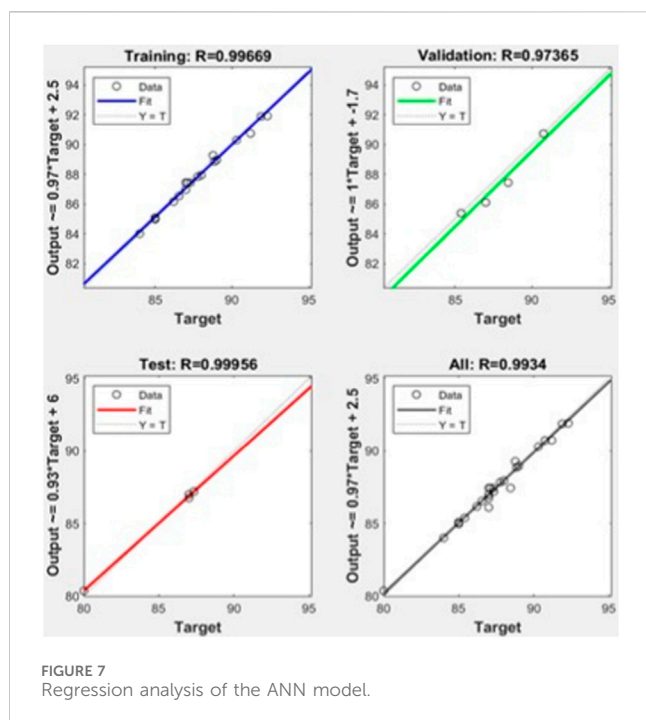


Figure 6E illustrates the increase in yield as the catalyst concentration and speed of stirring are increased, while the methanol concentration and reaction duration remain constant. The increased reactant levels and improved mixing, which result in an increase in reaction kinetics, are the causes of this increment in yield.

Increasing the time of reaction and speed of stirring leads to an escalation in the yield, as shown in Figure 6F, when the catalyst content of 12.5 Wt% and the methanol-to-oil volumetric concentration (%V/V) of 55% are kept constant. The higher yields are produced when reactions last longer because more reactants are transformed into products. The development of by-products and a lower yield, however, might occur when the reaction time is too long for the optimal value (Tamjidi et al., 2021).

3.4 Yield optimization using the ANN model

The ANN was also used to predict the results with the complete integration proposed by RSM. Three layers of neurons have been used in a feedforward backpropagation algorithm in this ANN technique. Input, hidden, and output layers are tansig, tansig, and purelin with 3, 10, and 1 neurons, respectively. When the MSE approaches 0.04761, the maximum yield obtained at this point is 92.4048%.

3.4.1 ANN training

The feedforward ANN model has been employed for training in using the data given in Table 4. Weight values and bias were updated using the “trainlm” function. The epochs were made up to 1,000, and the performance parameter mean square error (MSE) was used.

The central hidden layer neurons have been changed until the MSE gets reduced to 0.04761. Then, the trained ANN was used to

TABLE 6 Statistical data analysis.

Statistical tools	RSM	ANN
R^2	0.9951	0.9969
MSE	0.10	0.05
RMSE	0.31	0.21
SEP	0.36	0.25

determine the yield % for optimized parameter combinations as proposed by RSM.

3.4.2 Artificial neural network simulation

Conclusively, the trained network forecasts the outcomes (i.e., % biodiesel yields). Figure 7 evidently expresses the results of the yield by both ANN and practical experimentation. Both are almost the same, making sure that the RSM was efficient.

3.5 Statistical data analysis

The RSM and ANN performances have been shown in Table 6 using statistical data analysis. The coefficient of determination, i.e., R^2 , for both RSM and ANN models approaches 1, which indicates that the models are fit. The calculated MSE and RMSE values were greater for the RSM (0.10, 0.31) than were for the ANN (0.05, 0.21), respectively. The standard error of prediction for the RSM and ANN is 0.36 and 0.25, respectively. Considering the results of the statistical assessment, it has been determined that the ANN has more appropriate results than the RSM regarding prediction and accuracy. The significantly higher R^2 value of 0.9969 and the notably lower RMSE value of 0.21 observed in the ANN model, as opposed to the RSM model with an R^2 of 0.9951 and RMSE of 0.31, signify a stronger fit for the ANN than for the RSM model.

3.6 Characterization of biodiesel

The physicochemical properties of LSO B100 (100% biodiesel) were evaluated, and their results were compared with another biodiesel (sourced from WCO) and diesel. The D6751 and EN 14214 standards have been used to validate the physicochemical properties in the acceptable ranges. The characterization of biodiesel also includes the measurement of the properties that include kinematic viscosity at 40°C, density at 15°C, cetane number, calorific value, flash point, oxidative stability, and the cold flow properties, i.e., cold filter plugging point (CFPP), cloud point (CP), and pour point (PP), as shown in Table 7. It was observed that these values are within the suggested standard ranges. Thus, the produced biodiesel can replace petroleum diesel.

The optimized LSO B100 has a kinematic viscosity of 4.4 mm²/s, which is lower than that of the biodiesel produced from the WCO but higher than that of diesel, and the density (875 kg/m³) at 15°C is higher than that for both WCO biodiesel and diesel but satisfies the ASTM and EN standards. So, the LSO B100 has promising lubricating characteristics. The LSO B100 has an acid value of 0.25 mg KOH/g, which is within the range of the acceptable limit.

The LSO B100 has a calorific value of 38.80 MJ/kg, which is less than that for diesel, which has 45.36 MJ/kg. The flash point of the LSO

TABLE 7 Physicochemical properties of biodiesel produced from *Litchi chinensis* seed oil.

Properties	Units	Waste cooking oil biodiesel Milano et al. (2018)	Diesel Mujtaba et al. (2020)	LSO B100 (Author's)	ASTM D6751	EN 14214
Density at 15°C	kg/m ³	862.1	839.4	875	870–900	860–900
Kinematic viscosity at 40°C	mm ² /s	5.01	2.87	4.4	1.9–6	3.5–5
Cetane no.		61	48.50	53.2	>47	>51
Acid value	mg KOH/ g	0.13	0.15	0.25	<0.50	0.50
Calorific value	MJ/kg	38.76	45.67	38.8	—	—
Flash point	°C	154	78.50	175	>130	>120
Oxidative stability	h	4.61	13.20	6.1	3 h	6 h
Cloud point	°C	2	2	6.59	–3 to 12	—
Pour point	°C	12	2	0.3	–15 to 16	—
Cold filter plugging point	°C	7	0	–2.34	19 (max)	—

TABLE 8 Fatty acid composition of *Litchi chinensis* seed oil biodiesel.

Peak No	Compound	Structure	RT (min)	Composition (%)
1	Methyl tetradecanoate (myristic acid)	C14:0	15.466	0.37
2	Hexadecanoic acid, methyl ester (palmitic acid)	C16:0	17.909	22.02
3	Octadecadienoic acid, methyl ester (linoleic acid)	C18:2	20.243	33.44
4	Octadecenoic acid (oleic acid)	C18:1	20.357	40.24
5	Octadecanoic acid (stearic acid methyl ester)	C18:0	20.708	3.19
6	Eicosanoic acid, methyl ester (arachidic acid)	C20:0	23.723	0.70
Saturated (%), = 26.28				
Unsaturated (%) = 73.72				
Total (%) = 100				

B100 is 175°C, and it is quite higher than that for diesel and WCO biodiesel but satisfies the ASTM and EN standards. The higher flash point for LSO B100 reduces the safety risks as the biodiesel gets exposed to an ignition source. The pour point, cloud point, and cold filter plugging point for LSO B100 are 0.3, 6.59, and –2.34°C, respectively, which indicates that the LSO B100 is fit for utilization in cold environmental areas. The oxidative stability of LSO B100 is 6.1 h at 110°C, which is higher than that for WCO biodiesel. The cetane no. of LSO B100 (53.2) satisfies the limits of both the standards.

3.7 Composition of biodiesel sourced from *Litchi chinensis* seed oil

The composition shows that the presence of unsaturated fatty acids is higher (73.72%) than that of saturated fatty acids (26.28%), which implies that the produced biodiesel will have good cold flow

properties. Table 8 shows the percentage (area %) contents of long-chain elements.

The major content of the biodiesel is covered by oleic acid methyl ester (40.24%), followed by octadecanoic acid (stearic acid methyl ester, 33.44%). The larger quantity of unsaturated fatty acids shows that the *Litchi chinensis* seed oil biodiesel (B100) has good cold flow properties.

3.8 Comparison of energy consumption by microwave-assisted reaction and conventional reaction

The energy intake of the Dawlance DW-295 microwave-assisted reactor was noted for 100 mL of the LSO mixture, with 2 min of preheating, and with 6, 7, and 10 min of reaction time. The energy consumed by the microwave was 100, 111, and 150 kJ for the reaction times of 6, 7, and 10 min, respectively. The 260-W reactor required

60 min to preheat the 100 mL of mixture to 65°C; moreover, the reaction was complete in 20 min. So, the conventional reactor consumes 1,248 kJ of energy.

Because it has been observed that the time required for preheating in the case of the conventional process is substantially longer than that required for the microwave-assisted one, the power consumption is also higher in the case of the conventional method for biodiesel production. Therefore, it can be assumed that the microwave-assisted reaction for biodiesel synthesis is far better than the conventional method.

4 Conclusion

The microwave-assisted, extracted KOH-catalyzed transesterification reaction was implemented to produce biodiesel from *Litchi chinensis* seed oil. KOH, as a catalyst, was extracted from potato waste. The LSO has an FFA content of 2.5%, which was reduced to 0.504 mg KOH/g after microwave-assisted transesterification. The yield optimization was carried out using two methods—RSM and ANN. The maximum yields of biodiesel (B100) were predicted to be 93.27% with the RSM and 92.40% with the ANN, using the operating parameters of catalyst loading of 15% (W/W), a methanol concentration of 70% (%V/V), a stirring speed of 700 RPM, and a reaction speed of 8 min. The practical biodiesel yield obtained was 92.90%. It has been observed that the characterization of LSO B100 biodiesel satisfies the fuel requirements specified in the standards—ASTM D6751 and EN 14214. The GCMS analysis demonstrated the free fatty acid composition of LSO biodiesel (B100). The RSM and ANN were both identified as smarter tools with no broader iterations for solving differential equations. The results of both—RSM and ANN—are close to practical results, with inaccuracies of 0.003% and 0.005%, respectively. The developed models in this study are validated and can estimate the yield of biodiesel. The application of a microwave speeds up the transesterification process, which considerably decreases the time for completion of the reaction to 8 min when compared to the conventional method, which has an approximate reaction time of 80 min. The *Litchi chinensis* seed oil B100 biodiesel synthesized through microwave-assisted transesterification offers a more viable edge regarding time and consumption of energy.

Data availability statement

The original contributions presented in the study are included in the article/Supplementary material; further inquiries can be directed to the corresponding authors.

Author contributions

TA: Conceptualization, formal analysis, investigation, manuscript writing—original draft, review, and editing. FN:

Funding acquisition, investigation, project administration, supervision, and manuscript writing—review and editing. SI: Conceptualization, data curation, formal analysis, funding acquisition, project administration, resources, and manuscript writing—review and editing. MM: Data curation, methodology, resources, validation, visualization, and manuscript writing—review and editing. YF: Funding acquisition, project administration, resources, and manuscript writing—review and editing. MK: Investigation, resources, visualization, and manuscript writing—review and editing. GU: Formal analysis, investigation, visualization, and manuscript writing—review and editing. MF: writing—review and editing.

Funding

The authors declare that financial support was received for the research, authorship, and/or publication of this article. The authors extend their appreciation to the Researchers Supporting Project number (RSPD2023R698), King Saud University, Riyadh, Saudi Arabia for funding this research work.

Acknowledgments

The authors extend their appreciation to the Researchers Supporting Project number (RSPD2023R698), King Saud University, Riyadh, Saudi Arabia for funding this research work. This research work is part of the project supported by Higher Education Commission Pakistan Project number (NRPU 20-12879/NRPU/R&D/HEC/2020).

Conflict of interest

The authors declare that the research was conducted in the absence of any commercial or financial relationships that could be construed as a potential conflict of interest.

The authors declare that they were an editorial board member of Frontiers at the time of submission. This had no impact on the peer review process and the final decision.

Publisher's note

All claims expressed in this article are solely those of the authors and do not necessarily represent those of their affiliated organizations, or those of the publisher, editors, and reviewers. Any product that may be evaluated in this article, or claim that may be made by its manufacturer, is not guaranteed or endorsed by the publisher.

References

- Ahmad, G., Imran, S., Farooq, M., Shah, A. N., Anwar, Z., Rehman, A. U., et al. (2023). Biodiesel production from waste cooking oil using extracted catalyst from plantain banana stem via RSM and ANN optimization for sustainable development. *Sustainability* 15 (18), 13599. doi:10.3390/su151813599
- Amini, M., Younesi, H., Bahramifar, N., Lorestani, A. A. Z., Ghorbani, F., Daneshi, A., et al. (2008). Application of response surface methodology for optimization of lead biosorption in an aqueous solution by *Aspergillus Niger*. *J. Hazard. Mater.* 154 (1–3), 694–702. doi:10.1016/j.jhazmat.2007.10.114

- Amran, Y. H. A., Amran, Y. H. M., Alyousef, R., and Alabduljabbar, H. (2020). Renewable and sustainable energy production in Saudi Arabia according to Saudi Vision 2030; Current status and future prospects. *J. Clean. Prod.* 247, 119602. doi:10.1016/j.jclepro.2019.119602
- Azad, A., Rasul, M. G., Khan, M. M. K., Sharma, S. C., and Islam, R. (2015). Prospect of Moringa seed oil as a sustainable biodiesel fuel in Australia: a review. *Procedia Eng.* 105, 601–606. doi:10.1016/j.proeng.2015.05.037
- Banković-Ilić, I. B., Stamenković, O. S., and Veljković, V. B. (2012). Biodiesel production from non-edible plant oils. *Renew. Sustain. Energy Rev.* 16 (6), 3621–3647. doi:10.1016/j.rser.2012.03.002
- Beals, K. A. (2019). Potatoes, nutrition and health. *Am. J. potato Res.* 96 (2), 102–110. doi:10.1007/s12230-018-09705-4
- Betiku, E., and Adepoju, T. F. (2013). Methanolysis optimization of sesame (*Sesamum indicum*) oil to biodiesel and fuel quality characterization. *Int. J. Energy Environ. Eng.* 4 (1), 9–8. doi:10.1186/2251-6832-4-9
- Cheng, Z., Guo, Z., Fu, P., Yang, J., and Wang, Q. (2021). New insights into the effects of methane and oxygen on heat/mass transfer in reactive porous media. *Int. Commun. Heat Mass Transf.* 129, 105652. doi:10.1016/j.icheatmasstransfer.2021.105652
- Chung, N. T., Choi, S.-R., and Kim, J.-G. (2022). Comparison of response surface methodologies and artificial neural network approaches to predict the corrosion rate of carbon steel in soil. *J. Electrochem. Soc.* 169 (5), 051503. doi:10.1149/1945-7111/ac700d
- Cormos, C.-C., Vatopoulos, K., and Tzimas, E. (2013). Assessment of the consumption of water and construction materials in state-of-the-art fossil fuel power generation technologies involving CO₂ capture. *Energy* 51, 37–49. doi:10.1016/j.energy.2012.12.050
- Degfie, T. A., Mamo, T. T., and Mekonnen, Y. S. (2019). Optimized biodiesel production from waste cooking oil (WCO) using calcium oxide (CaO) nano-catalyst. *Sci. Rep.* 9 (1), 18982. doi:10.1038/s41598-019-55403-4
- Duan, X., Wu, G., and Jiang, Y. (2007). Evaluation of the antioxidant properties of litchi fruit phenolics in relation to pericarp browning prevention. *Molecules* 12 (4), 759–771. doi:10.3390/12040759
- Efevbokhan, V. E., Abiodun, O. J., and Eric, K. E. (2016). Extraction and use of potassium hydroxide from ripe plantain peels ash for biodiesel production. *J. Biobased Mater. Bioenergy* 10 (1), 1–9. doi:10.1166/jbmb.2016.1567
- Elkelawy, M., Alm-Eldin Bastawissi, H., Esmaeil, K. K., Radwan, A. M., Panchal, H., Sadasivuni, K. K., et al. (2019). Experimental studies on the biodiesel production parameters optimization of sunflower and soybean oil mixture and DI engine combustion, performance, and emission analysis fueled with diesel/biodiesel blends. *Fuel* 255, 115791. doi:10.1016/j.fuel.2019.115791
- Encinar, J. M., Pardal, A., and Martínez, G. (2012). Transesterification of rapeseed oil in subcritical methanol conditions. *Fuel Process. Technol.* 94 (1), 40–46. doi:10.1016/j.fuproc.2011.10.018
- Fattah, I. M. R., Masjuki, H. H., Kalam, M. A., Mofijur, M., and Abedin, M. J. (2014b). Effect of antioxidant on the performance and emission characteristics of a diesel engine fueled with palm biodiesel blends. *Energy Convers. Manag.* 79, 265–272. doi:10.1016/j.enconman.2013.12.024
- Fattah, I. M. R., Masjuki, H. H., Kalam, M. A., Wakil, M. A., Ashraful, A. M., and Shahir, S. A. (2014a). Experimental investigation of performance and regulated emissions of a diesel engine with *Calophyllum inophyllum* biodiesel blends accompanied by oxidation inhibitors. *Energy Convers. Manag.* 83, 232–240. doi:10.1016/j.enconman.2014.03.069
- Fetimi, A., Dâas, A., Merouani, S., Alswieleh, A. M., Hamachi, M., Hamdaoui, O., et al. (2022). Predicting emulsion breakdown in the emulsion liquid membrane process: optimization through response surface methodology and a particle swarm artificial neural network. *Chem. Eng. Process. Intensif.* 176, 108956. doi:10.1016/j.cep.2022.108956
- Fukuda, H., Kondo, A., and Noda, H. (2001). Biodiesel fuel production by transesterification of oils. *J. Biosci. Bioeng.* 92 (5), 405–416. doi:10.1016/s1389-1723(01)80288-7
- Gupta, A., Viltres, H., and Gupta, N. K. (2020). Sono-adsorption of organic dyes onto CoFe₂O₄/Graphene oxide nanocomposite. *Surfaces Interfaces* 20, 100563. doi:10.1016/j.surfin.2020.100563
- Hansen, J., Sato, M., Ruedy, R., Lo, K., Lea, D. W., and Medina-Elizade, M. (2006). Global temperature change. *Proc. Natl. Acad. Sci.* 103 (39), 14288–14293. doi:10.1073/pnas.0606291103
- Helmi, M., Tahvildari, K., Hemmati, A., and Safekordi, A. (2021). Phosphomolybdc acid/graphene oxide as novel green catalyst using for biodiesel production from waste cooking oil via electrolysis method: optimization using with response surface methodology (RSM). *Fuel* 287, 119528. doi:10.1016/j.fuel.2020.119528
- Ighose, B. O., Adeleke, I. A., Damos, M., Junaid, H. A., Okpalaek, K. E., and Betiku, E. (2017). Optimization of biodiesel production from *Thevetia peruviana* seed oil by adaptive neuro-fuzzy inference system coupled with genetic algorithm and response surface methodology. *Energy Convers. Manag.* 132, 231–240. doi:10.1016/j.enconman.2016.11.030
- Ilkilic, C., and Behçet, R. (2010). The reduction of exhaust emissions from a diesel engine by using biodiesel blend. *Energy Sources, Part A recover. Util. Environ. Eff.* 32 (9), 839–850. doi:10.1080/15567030802606269
- Ishola, N. B., Okeleye, A. A., Osunleke, A. S., and Betiku, E. (2019). Process modeling and optimization of sorrel biodiesel synthesis using barium hydroxide as a base heterogeneous catalyst: appraisal of response surface methodology, neural network and neuro-fuzzy system. *Neural Comput. Appl.* 31, 4929–4943. doi:10.1007/s00521-018-03989-7
- Jalali, S. M. J., Ahmadian, S., Khosravi, A., Shafie-khah, M., Nahavandi, S., and Catalão, J. P. S. (2021). A novel evolutionary-based deep convolutional neural network model for intelligent load forecasting. *IEEE Trans. Ind. Inf.* 17 (12), 8243–8253. doi:10.1109/tii.2021.3065718
- Kabeyi, M. J. B., and Olanrewaju, O. A. (2022). Sustainable energy transition for renewable and low carbon grid electricity generation and supply. *Front. Energy Res.* 9, 1032. doi:10.3389/fenrg.2021.743114
- Kan, Y., Kan, H., Bai, Y., Zhang, S., and Gao, Z. (2023b). Effective and environmentally safe self-antimildew strategy to simultaneously improve the mildew and water resistances of soybean flour-based adhesives. *J. Clean. Prod.* 392, 136319. doi:10.1016/j.jclepro.2023.136319
- Kan, Y., Li, J., Zhang, S., and Gao, Z. (2023a). Novel bridge assistance strategy for tailoring crosslinking networks within soybean-meal-based biocomposites to balance mechanical and biodegradation properties. *Chem. Eng. J.* 472, 144858. doi:10.1016/j.cej.2023.144858
- Kolakoti, A. (2020). Optimization of biodiesel production from waste cooking sunflower oil by taguchi and ann techniques. *J. Therm. Eng.* 6 (5), 712–723. doi:10.18186/thermal.796761
- Laskar, I. B., Deshmukhya, T., Biswas, A., Paul, B., Changmai, B., Gupta, R., et al. (2022). Utilization of biowaste-derived catalysts for biodiesel production: process optimization using response surface methodology and particle swarm optimization method. *Energy Adv.* 1 (5), 287–302. doi:10.1039/d2ya00011c
- Li, H., Li, G., and Li, L. (2023). Comparative investigation on combustion characteristics of ADN-based liquid propellants in inert gas and oxidizing gas atmospheres with resistive ignition method. *Fuel* 334, 126742. doi:10.1016/j.fuel.2022.126742
- Lin, H., Zhao, B., Liu, D., and Alippi, C. (2020). Data-based fault tolerant control for affine nonlinear systems through particle swarm optimized neural networks. *IEEE/CAA J. Autom. Sin.* 7 (4), 954–964. doi:10.1109/jas.2020.1003225
- Liu, L., Tang, Y., and Liu, D. (2022a). Investigation of future low-carbon and zero-carbon fuels for marine engines from the view of thermal efficiency. *Energy Rep.* 8, 6150–6160. doi:10.1016/j.egy.2022.04.058
- Liu, L., Wu, Y., Wang, Y., Wu, J., and Fu, S. (2022b). Exploration of environmentally friendly marine power technology -ammonia/diesel stratified injection. *J. Clean. Prod.* 380, 135014. doi:10.1016/j.jclepro.2022.135014
- Maran, J. P., and Priya, B. (2015). Comparison of response surface methodology and artificial neural network approach towards efficient ultrasound-assisted biodiesel production from muskmelon oil. *Ultrason. Sonochem.* 23, 192–200. doi:10.1016/j.ultrsonch.2014.10.019
- Milano, J., Ong, H. C., Masjuki, H., Silitonga, A., Chen, W. H., Kusumo, F., et al. (2018). Optimization of biodiesel production by microwave irradiation-assisted transesterification for waste cooking oil-*Calophyllum inophyllum* oil via response surface methodology. *Energy Convers. Manag.* 158, 400–415. doi:10.1016/j.enconman.2017.12.027
- Moser, B. R. (2008). Influence of blending canola, palm, soybean, and sunflower oil methyl esters on fuel properties of biodiesel. *Energy and Fuels* 22 (6), 4301–4306. doi:10.1021/ef800588x
- Mujtaba, M. A., Masjuki, H., Kalam, M., Ong, H. C., Gul, M., Farooq, M., et al. (2020). Ultrasound-assisted process optimization and tribological characteristics of biodiesel from palm-sesame oil via response surface methodology and extreme learning machine-Cuckoo search. *Renew. Energy* 158, 202–214. doi:10.1016/j.renene.2020.05.158
- Ofoeule, A. U., Esonye, C., Onukwuli, O. D., Nwaeze, E., and Ume, C. S. (2019). Modeling and optimization of African pear seed oil esterification and transesterification using artificial neural network and response surface methodology comparative analysis. *Ind. Crops Prod.* 140, 111707. doi:10.1016/j.indcrop.2019.111707
- Palma, V., Barba, D., Cortese, M., Martino, M., Renda, S., and Meloni, E. (2020). Microwaves and heterogeneous catalysis: a review on selected catalytic processes. *Catalysts* 10 (2), 246. doi:10.3390/catal10020246
- Pandey, R. K., Rehman, A., Sarviya, R. M., and Dixit, S. (2010). Automobile emission reduction and environmental protection through use of green renewable fuel. *Hydro Nepal J. Water, Energy Environ.* 7, 65–70. doi:10.3126/hn.v7i0.4240
- Patil, P. D., and Deng, S. (2009). Optimization of biodiesel production from edible and non-edible vegetable oils. *Fuel* 88 (7), 1302–1306. doi:10.1016/j.fuel.2009.01.016
- Rahul Soosai, M., Moorthy, I. M. G., Varalakshmi, P., and Yonas, C. J. (2022). Integrated global optimization and process modelling for biodiesel production from non-edible silk-cotton seed oil by microwave-assisted transesterification with heterogeneous calcium oxide catalyst. *J. Clean. Prod.* 367, 132946. doi:10.1016/j.jclepro.2022.132946

- Rajendra, M., Jena, P. C., and Raheman, H. (2009). Prediction of optimized pretreatment process parameters for biodiesel production using ANN and GA. *Fuel* 88 (5), 868–875. doi:10.1016/j.fuel.2008.12.008
- Rizwanul Fattah, I. M., Ong, H. C., Mahlia, T. M. I., Mofijur, M., Silitonga, A. S., Rahman, S. M. A., et al. (2020). State of the art of catalysts for biodiesel production. *Front. Energy Res.* 8, 101. doi:10.3389/fenrg.2020.00101
- Sahabdheen, A. B., and Arivarasu, A. (2020). Synthesis and characterization of reusable heteropoly acid nanoparticles for one step biodiesel production from high acid value waste cooking oil—Performance and emission studies. *Mater. Today Proc.* 22, 383–392. doi:10.1016/j.matpr.2019.07.249
- Silitonga, A. S., Mahlia, T., Kusumo, F., Dharma, S., Sebayang, A., Sembiring, R., et al. (2019). Intensification of Reutealis trisperma biodiesel production using infrared radiation: simulation, optimisation and validation. *Renew. Energy* 133, 520–527. doi:10.1016/j.renene.2018.10.023
- Tamjidi, S., Esmaili, H., and Moghadas, B. K. (2021). Performance of functionalized magnetic nanocatalysts and feedstocks on biodiesel production: a review study. *J. Clean. Prod.* 305, 127200. doi:10.1016/j.jclepro.2021.127200
- Tran-Nguyen, P. L., Ong, L. K., Go, A. W., Ju, Y., and Angkawijaya, A. E. (2020). Non-catalytic and heterogeneous acid/base-catalyzed biodiesel production: recent and future developments. *Asia-Pacific J. Chem. Eng.* 15 (3), e2490. doi:10.1002/apj.2490
- Vijay Kumar, M., Veeresh Babu, A., and Ravi Kumar, P. (2019). Producing biodiesel from crude Mahua oil by two steps of transesterification process. *Aust. J. Mech. Eng.* 17 (1), 2–7. doi:10.1080/14484846.2017.1412243
- Wang, B., Gupta, R., Bei, L., Wan, Q., and Sun, L. (2023b). A review on gasification of municipal solid waste (MSW): syngas production, tar formation, mineral transformation and industrial challenges. *Int. J. Hydrogen Energy* 48, 26676–26706. doi:10.1016/j.ijhydene.2023.03.086
- Wang, Y., Wang, Q., Li, Y., Wang, H., Gao, Y., Sun, Y., et al. (2023a). Impact of incineration slag co-disposed with municipal solid waste on methane production and methanogens ecology in landfills. *Bioresour. Technol.* 377, 128978. doi:10.1016/j.biortech.2023.128978
- Wang, Z., Wang, Q., Jia, C., and Bai, J. (2022). Thermal evolution of chemical structure and mechanism of oil sands bitumen. *Energy (Oxford)* 244, 123190. doi:10.1016/j.energy.2022.123190
- Wu, H., and Zhao, J. (2020). Self-adaptive deep learning for multimode process monitoring. *Comput. Chem. Eng.* 141, 107024. doi:10.1016/j.compchemeng.2020.107024
- Yang, X., Liu, K., Han, X., Xu, J., Bian, M., Zheng, D., et al. (2023). Transformation of waste battery cathode material LiMn₂O₄ into efficient ultra-low temperature NH₃-SCR catalyst: proton exchange synergistic vanadium modification. *J. Hazard. Mater.* 459, 132209. doi:10.1016/j.jhazmat.2023.132209
- Yuan, X., Liu, J., Zeng, G., Shi, J., Tong, J., and Huang, G. (2008). Optimization of conversion of waste rapeseed oil with high FFA to biodiesel using response surface methodology. *Renew. Energy* 33 (7), 1678–1684. doi:10.1016/j.renene.2007.09.007
- Yusoff, M. N. A. M., Zulkifli, N., Sukiman, N., Kalam, M., Masjuki, H., Syahir, A., et al. (2022). Microwave irradiation-assisted transesterification of ternary oil mixture of waste cooking oil – Jatropha curcas – palm oil: optimization and characterization. *Alex. Eng. J.* 61 (12), 9569–9582. doi:10.1016/j.aej.2022.03.040
- Yusoff, M. N. A. M., Zulkifli, N. W. M., Sukiman, N. L., Chyuan, O. H., Hassan, M. H., Hasnul, M. H., et al. (2021). Sustainability of palm biodiesel in transportation: a review on biofuel standard, policy and international collaboration between Malaysia and Colombia. *Bioenergy Res.* 14, 43–60. doi:10.1007/s12155-020-10165-0
- Zhang, D., Quantick, P. C., and Grigor, J. M. (2000). Changes in phenolic compounds in Litchi (Litchi chinensis Sonn.) fruit during postharvest storage. *Postharvest Biol. Technol.* 19 (2), 165–172. doi:10.1016/s0925-5214(00)00084-3
- Zhang, H., Li, H., Pan, H., Wang, A., Souzanchi, S., Xu, C. C., et al. (2018). Magnetically recyclable acidic polymeric ionic liquids decorated with hydrophobic regulators as highly efficient and stable catalysts for biodiesel production. *Appl. Energy* 223, 416–429. doi:10.1016/j.apenergy.2018.04.061
- Zhang, J., Chen, S., Yang, R., and Yan, Y. (2010). Biodiesel production from vegetable oil using heterogeneous acid and alkali catalyst. *Fuel* 89 (10), 2939–2944. doi:10.1016/j.fuel.2010.05.009
- Zhang, T., Li, Y., Li, Y., Sun, S., and Gao, X. (2020). A self-adaptive deep learning algorithm for accelerating multi-component flash calculation. *Comput. Methods Appl. Mech. Eng.* 369, 113207. doi:10.1016/j.cma.2020.113207